HHS Public Access

Author manuscript

Dev Dyn. Author manuscript; available in PMC 2022 July 08.

Published in final edited form as:

Dev Dyn. 2021 October ; 250(10): 1463–1476. doi:10.1002/dvdy.327.

The *Mafb* cleft-associated variant H131Q is not required for palatogenesis in the mouse

Brian J. Paul[1], **Kristina J. Palmer**[2], **Lindsey Rhea**[1], **Melissa Carlson**[1], **Jocelyn C. Sharp**[2], **C. Herbert Pratt**[2], **Stephen A. Murray**[2], **Martine Dunnwald**[1]

[1]Department of Anatomy and Cell Biology, The University of Iowa, Iowa City, Iowa

[2]The Jackson Laboratory, Bar Harbor, Maine

Abstract

Background: Orofacial clefts (OFCs) are common birth defects with complex etiology. Genome wide association studies for OFC have identified SNPs in and near *MAFB*. MAFB is a transcription factor critical for structural development of digits, kidneys, skin, and brain. *MAFB* is also expressed in the craniofacial region. Previous sequencing of *MAFB* in a Filipino population revealed a novel missense variant significantly associated with an increased risk for OFC. This *MAFB* variant, leading to the amino acid change H131Q, was knocked into the mouse *Mafb*, resulting in the $Mafb^{H131Q}$ allele. The $Mafb^{H131Q}$ construct was engineered to allow for deletion of *Mafb* ($Mafb^{del}$).

Results: $Mafb^{del/del}$ animals died shortly after birth. Conversely, $Mafb^{H131Q/H131Q}$ mice survived into adulthood at Mendelian ratios. $Mafb^{del/del}$ and $Mafb^{H131Q/H131Q}$ heads exhibited normal macroscopic and histological appearance at all embryonic time points evaluated. The periderm was intact based on expression of keratin 6, p63, and E-cadherin. Despite no effect on craniofacial morphogenesis, H131Q inhibited the Mafb-dependent promoter activation of Arhgap29 in palatal mesenchymal, but not ectodermal-derived epithelial cells in a luciferase assay.

Conclusions: Mafb is dispensable for murine palatogenesis *in vivo*, and the cleft-associated variant H131Q, despite its lack of morphogenic effect, altered the expression of *Arhgap29* in a cell-dependent context.

Keywords

craniofacial; development; Mafb; mouse; mutation

Correspondence: Martine Dunnwald, Anatomy and Cell Biology, The University of Iowa, Iowa City, IA, 52242, USA. martine-dunnwald@uiowa.edu.

AUTHOR CONTRIBUTIONS

Brian Paul: Conceptualization; data curation; formal analysis; methodology; writing-original draft; writing-review & editing. **Kristina Palmer:** Investigation; methodology; writing-review & editing. **Lindsey Rhea:** Conceptualization; formal analysis; investigation; writing-review & editing. **Melissa Carlson:** Formal analysis; methodology. **Jocelyn Sharp:** Methodology. **Herbert Pratt:** Methodology. **Stephen Murray:** Conceptualization; funding acquisition; methodology; resources; writing-review & editing. **Martine Dunnwald:** Conceptualization; data curation; formal analysis; funding acquisition; investigation; methodology; project administration; resources; supervision; writing-original draft; writing-review & editing.

Mafb, a transcription factor associated with cleft lip and palate in human, is not required in the mouse.

1 | INTRODUCTION

Orofacial clefts (OFCs) are among the most common structural birth defects, affecting 1 in 700 live births.[1] The etiology is complex, with contributions from genetic and environmental factors. Over decades of research, many genes have been identified causing and contributing to syndromic and sporadic OFCs (for review,[1–3]). Multiple gene discovery approaches have been used including linkage analysis,[4] genomic rearrangements, candidate genes,[5] and more recently genome-wide association studies (GWAS) and whole exome sequencing.[6–10] One locus replicated in multiple independent studies in diverse ethnic populations is located on the chromosomal region 20q12, near or in *MAF* bZIP transcription factor B (*MAFB*).[7,11–16] Targeted sequencing of the single *MAFB* exon and conserved elements 3′ of *MAFB* identified a rare missense variant in a highly conserved histidine leading to a glutamine at position 131 (Figure 1A) which is predicted to alter the protein structure and function by Polyphen2.[17] H131Q was present in 3.5% of a Filipino population with non-syndromic cleft lip and/or palate (NSCL/P) and 0.7% of unaffected controls, demonstrating its significant association with OFC.[2,7] However, the functional contribution of this variant to craniofacial development is currently unknown.

The MAF family of transcription factors consists of both large (including MAFB and c-MAF) and small MAFs, all of which share a C-terminal bZIP domain and leucine-rich protein-binding domain.[18,19] The N-terminus is only present in the large MAF proteins and contains a transcriptional activation domain inducing MAF target gene transcription by recruiting other transcriptional regulators. The large MAFs have been implicated in a variety of differentiation processes, during development of gonads, hematopoietic and lymphatic systems, hindbrain, pancreatic islets, kidney, and ectoderm.[18–26]

In vivo, the earliest study of *Mafb* came from the *kreisler* (*kr*) mutation, which was discovered following mouse x-ray mutagenesis in 1942.[27] The *kreisler* (Kreis = circle in German) mutation is a radiation-induced chromosomal inversion that separates *Mafb* from a putative distal enhancer. *Kreisler* mice are characterized by their circling or “dancing” movement due to hindbrain and inner ear developmental defects. The etiologic gene of this mutation was later determined to be *Mafb*,[18] which has since been described extensively in the development of the hindbrain as a controller of rhombomere segmentation and cardiac neural crest cell migration.[28,29] Multiple murine alleles have been generated over the years, including complete loss of function,[24,26] several tissue-specific deletions,[30,31] overexpression of *Mafb*,[32] and an allele harboring a human variant.[33] *Mafb* loss-of-function leads to neonatal lethality due to respiratory failure,[22] failure of renal development and macrophage differentiation.[22,24] In addition, mice lacking *Mafb* present with defects in both abducens nerve and lateral rectus muscle development.[34] However, the biological consequences of *Mafb* loss on palatal development have never been addressed.

To determine the role of *Mafb* in palatal development, we generated two novel *Mafb* alleles: one in which the H131Q cleft associated variant was engineered into the *Mafb* gene, and one in which *Mafb* was deleted following Cre-loxP recombination of the previous H131Q allele. We report that mice homozygous for the *Mafb* H131Q and null alleles exhibit proper palatogenesis *in vivo*.

2 | RESULTS

2.1 | A NSCL/P patient-associated Mafb^{H131Q} allele results in normal Mendelian ratios, while Mafb^{del} is homozygous lethal at birth in mice

In order to evaluate the function of MAFB and the cleft-associated H131Q variant[7] during craniofacial development, the single base-pair C to G change was engineered at position 782 of the gene sequence leading to the Mafb^{H131Q} allele. In addition, the entire single coding exon was flanked by *loxP* sites, and a deletion (null) allele was generated by crossing with a *Sox2-cre* (*Edil*$^{Tg(Sox2-cre)1Amc}$ (referred to as *Mafb*^{del}, Figure 1B). This strategy allowed for the direct comparison of altered *Mafb* alleles in closely-related mice in the C57 background. Heterozygous mice for both *Mafb*^{H131Q} and *Mafb*^{del} were viable in expected Mendelian ratios (Table 1) and did not present gross morphological abnormalities (Figure 1C). *Mafb*$^{H131Q/H131Q}$ were macroscopically indistinguishable from their wild-type and heterozygous counterparts and viable in expected Mendelian ratios (Table 1 and Figure 1C). However, although the *Mafb*$^{del/del}$ completed embryogenesis, they died shortly after birth (Table 1), as previously reported for other loss of function *Mafb* alleles.[22] The total number of embryos obtained from the *Mafb*^{del} intercross was slightly below the expected mouse litter size (average of five pups for *Mafb*$^{del/del}$ compared to average of six to seven pups for wild-type intercrosses), possibly due to poor parenting, yet no issues with fighting or aggression were noted. Loss of *Mafb* transcript was confirmed in *Mafb*$^{del/del}$ following RNA-sequencing of e18.5 skin. However, *Mafb* transcript was unaltered in *Mafb*$^{H131Q/H131Q}$ (Figure 1D and Table 2). Transcripts of other Maf family members were unchanged (Table 2). These data demonstrate that we successfully generated two novel murine *Mafb* alleles, including one in which we deleted the *Mafb* gene.

2.2 | Palatogenesis is not altered in Mafb$^{H131Q/H131Q}$ or Mafb$^{del/del}$ mice

The completion of palatogenesis is required for survival in mice, as cleft palate impairs suckling. As *Mafb*$^{de/del}$ mice died shortly after birth, we hypothesized that these animals would present with a cleft of their secondary palate. This hypothesis was also supported by human genetic association studies demonstrating the contribution of the *MAFB* locus to the etiology of orofacial clefting.[7,11–16] We performed serial coronal sections of e14.5 and e17.5 murine heads (Figure 2). By e14.5, over 70% of wild-type embryos presented with elevated palatal shelves and 40–60% of the shelves were in contact with each other (Table 3, Figure 2A). Three days later, palatogenesis was completed with the presence of a confluent mesenchymal bridge on the roof of the mouth, separating the oral from the nasal cavity (Figure 2D). We observed proper palatal morphogenesis at e14.5, and a confluent palatal bridge in *Mafb*^{H131QH131Q} mice at e17.5 (Figure 2B,E). We observed similar palatogenesis in *Mafb*$^{del/del}$ mice (Figure 2C,F). These data demonstrate that *Mafb* is dispensable for palatogenesis in the mouse.

2.3 | Oral epithelial morphogenesis is not altered in Mafb$^{H131Q/H131Q}$ or Mafb$^{del/del}$ mice

Although palatogenesis was not altered in *Mafb*$^{H131Q/H131Q}$ or *Mafb*$^{del/del}$ mice, other orofacial defects have been examined in association with OFC. Of interest to our study are intraoral adhesions as they were previously reported in several murine models of OFC, including mice heterozygous for *Irf6* and *Arhgap29*, two genes in the same gene regulatory

network as *Mafb*.[7,35,36] We used our previously developed adhesion assay[35,37] to evaluate oral epithelial contact in *Mafb*^{H131Q} and *Mafb*^{del} heterozygous and homozygous mice at e14.5. Our data show no significant increase in oral epithelial adhesions in any of the *Mafb* murine lines compared to wild types (Table 3, Figure 2G,H).

To further determine if *Mafb* levels alter oral epithelial morphogenesis, we performed immunostaining for key proteins involved in oral epithelial differentiation. At e14.5, the periderm is observed as a flat layer of ectodermally-derived cells covering the oral epithelium. In wild-type embryos, periderm cells express keratin (K) 6 and lack p63 (Figure 3A). Periderm cells also lack E-cadherin at their outermost plasma membrane ("apicolateral" side), yet show E-cadherin at their cell-cell junctions with other epithelial cells (Figure 3D,G,G′). Examination of *Mafb*$^{H131Q/H131Q}$ and *Mafb*$^{del/del}$ e14.5 coronal sections showed that these proteins were detected in a similar pattern to their wild-type littermates (Figure 3B,C,E,F,H,I,H′,I′). Thus, our data demonstrate that *Mafb* is dispensable for oral epithelial morphogenesis and periderm formation and function.

2.4 | MAFB H131Q alters ARHGAP29 promoter- and enhancer-driven activity in a cell-dependent context

ARHGAP29 is a RhoA GTPase Activating Protein contributing to OFC.[35,38] It was previously demonstrated that MAFB binds an *ARHGAP29* enhancer and promotes its transcriptional activity.[39] This binding was diminished in oral epithelial cell lines *in vitro* by a cleft-associated risk single nucleotide polymorphism (SNP) rs4147828 in the *ARHGAP29* enhancer.[39] Additionally, an MAFB ChIP-seq in cutaneous keratinocytes identified a peak in the *ARHGAP29* promoter indicating MAFB could also be regulating the transcription of *ARHGAP29* at its promoter (Figure 4A, B).[19] Although H131Q mutation did not affect palatogenesis *in vivo*, we asked whether it could affect the regulation of *ARHGAP29* in these contexts. The *ARHGAP29* promoter and enhancer were cloned upstream of the luciferase gene to measure transcriptional activity (Figure 4A,B). A mutant promoter was generated with the MAFB ChIP-seq peak and surrounding seven base pairs deleted by Around-the-horn mutagenesis as a negative control while the mutant enhancer with the cleft-associated risk SNP[39] was used as a "sensitized genetic background." In human embryonic palatal mesenchymal cells (HEPM), co-transfection of the *ARHGAP29* promoter or *ARHGAP29* enhancer with MAFB resulted in increased luciferase activity (Figure 4C,D). Co-transfection of the luciferase constructs with the MAFB H131Q failed to activate the promoter and inhibited the enhancer construct (Figure 4C,D). However, when we repeated these experiments in LS-8 cells, an ameloblast-like precursor murine cell line, we found that co-transfection of the *ARHGAP29* promoter with MAFB H131Q significantly increased luciferase activity, while wild-type MAFB did not, suggesting a potential gain of function (Figure 4E). Interestingly, there was no reduction in luciferase activity when the MAFB binding site was mutated from the promoter region, indicating that the overall effect of MAFB H131Q may not require binding to the *ARHGAP29* promoter in these cells and may interact with other basal transcription factors not present in HEPM cells (Figure 4E). Similar experiments with the *ARHGAP29* enhancer in LS-8 cells confirmed the ability of MAFB to promote *ARHGAP29* transcriptional activity as previously demonstrated in GMSM-K (human oral epithelial cells[39]). This effect was abrogated by the introduction

of the risk SNP on the *ARHGAP29* enhancer (Figure 4F). The MAFB H131Q variant, however, had no impact on this effect (Figure 4F). Collectively, these results indicate that the MAFB H131Q variant has differing effects on the activation of the *ARHGAP29* promoter and enhancer depending on cellular context. In human mesenchymal cells the H131Q variant abrogates MAFB function whereas in ectodermal-derived mouse cells, it significantly increases ARHGAP29 expression at its promoter even in the absence of the MAFB binding site, suggesting it may act as a gain of function mutation.

2.5 | $Arhgap29^{K326X/+};Mafb^{del/+}$ double heterozygotes exhibit proper palatogenesis

Based on our results, we hypothesized that *Arhgap29* and *Mafb* interact genetically *in vivo* during palatogenesis. We crossed $Arhgap29^{K326X/+}$ (a previously demonstrated functional null allele[35]) with $Mafb^{del/+}$ and obtained animals in the expected Mendelian ratios (Table 4). Interestingly, the average number of embryos per litter at e18.5 and P0 were low (about 6 pups per litter) similarly to what we observed with the $Mafb^{del/+} \times Mafb^{del/+}$ cross, suggesting a potential issue with the $Mafb^{del}$ dam. $Arhgap29^{K326X/+};Mafb^{del/+}$ were viable and did not exhibit any defect in palatogenesis at e18.5 or at birth (Table 4), suggesting that reduction of *Arhgap29* in $Mafb^{del}$ heterozygotes did not alter palatal development.

3 | DISCUSSION

In this study, we report the generation of a novel murine *Mafb* allele modified with a cleft-associated missense variant in a highly conserved histidine repeat domain. Phenotypic characterization of this mouse and its derived homozygous null mouse reveals that MAFB is dispensable for palatogenesis in the mouse. In humans, this same point mutation is associated with non-syndromic cleft lip and palate.[7] Additional SNPs in or around the *MAFB* chromosomal region have been associated with orofacial clefting in a variety of populations,[7,11–16] identifying this region, and potentially *MAFB*, as a genetic contributor to OFCs. This raises the question as to why the *MAFB* locus appears to contribute risk for OFC in human, yet complete loss of function of the mouse gene does not lead to a cleft lip and/or palate in this animal.

The potential contribution of *MAFB* to orofacial clefting was found through genetic association studies. These statistical analyses, powerful at identifying risk loci for complex traits, did not identify *MAFB* as the etiologic gene of these OFCs. In fact, in humans, heterozygous loss of function mutations in *MAFB* lead to Duane retraction syndrome (OMIM 617041[33,34]) and heterozygous missense mutations in this same gene caused multicentric carpotarsal osteolysis syndrome (OMIM 166300[40]). None of the patients with these syndromes were reported with OFCs, although other craniofacial abnormalities have been described in some multi carpotarsal osteolysis syndrome patients.[40] Therefore, it could be that genetic variations identified in *MAFB* in the context of cleft lip and/or palate are in linkage disequilibrium with other genetic variants which could account for the structural birth defect. Whole genome sequencing and deep genetic analyses would be required to test this hypothesis.

Alternatively, it is plausible that the GWAS loci in *MAFB* act by regulating nearby genes. Careful evaluation of the genome surrounding *MAFB* shows that the closest gene on the side

of the lead SNP (rs13041247) identified in the Filipino population is 1.8 million bases away from *MAFB*,[7] placing *MAFB* in some sort of "gene desert." However, distant enhancers have been previously reported, as far as millions bases from their regulatory target.[41] Previous GWAS signals have been identified in craniofacial enhancers. They include loci at chromosomes 1 and 8. The 8q24 locus is strongly associated with increased risk for non-syndromic cleft lip and/or palate in European populations. This 640 kb noncoding interval contains cis-acting enhancers that control *Myc* expression in the developing face.[42] The 1p22.1 locus includes signals near and in introns of the *ABCA4* gene. Expression analysis and mutation screening of *ABCA4* did not support a role for this gene in nonsyndromic cleft lip and/or palate, but investigation of the nearby gene *ARHGAP29* concluded that it was the etiologic gene.[38] Further functional studies demonstrated that this locus served as an enhancer for *ARHGAP29*, and that the SNP altered an MAFB binding site critical for the activity of the *ARHGAP29* enhancer to drive expression of this gene.[39] We replicated this result in our study with ectodermal-derived LS-8 cells, however, in neural crest-derived HEPM cells the risk SNP did not alter enhancer activity, indicating a tissue specific effect as would be expected of an enhancer.

With that in mind, we asked whether the *MAFB* H131Q variant would alter the expression of ARHGAP29. Our results confirmed that MAFB is an activator of *ARHGAP29* and highlight for the first time a functional role for the H131Q variant. MAFB H131Q variant abolished both the *ARHGAP29* promoter and enhancer-driven luciferase activity in neural crest-derived HEPM, and increased its promoter-driven activity in ectodermal-derived LS-8 cells with no effect on the enhancer-driven activity. These results suggest that H131Q may abrogate MAFB function in a cell line where MAFB has not been previously detected. In ectodermal-derived LS-8, it appears that the effect of MAFB and H131Q on the *ARHGAP29* promoter is not due to the binding of the promoter, as similar results were observed when this site was mutated. We speculate that this effect may be due to the presence of other ectodermal-specific factors, including binding of other transcription factors. It remains that RNAseq and protein analysis (data not shown) of ARHGAP29 levels in skin extracts at e18.5 did not demonstrate a change in ARHGAP29. A systematic investigation of spatial and temporal regulation of ARHGAP29 in our MAFB mutant would be warranted to explain this discrepancy. Because of this unique relationship between ARHGAP29 and MAFB, we hypothesized *MAFB* and *ARHGAP29* may interact *in vivo* leading to defective palatogenesis not observed with *Arhgap29* or *Mafb* heterozygotes alone. However, double heterozygous *Arhgap29;Mafb* animals proceeded through palatogenesis without any noticeable defects. Future crosses between $Mafb^{H131Q/H131Q}$ or $Mafb^{del/del}$ and $Arhgap29^{+/-}$ may provide a more sensitized background and lead to defective palatogenesis not observed in this study. It should also be noted that all the alleles were in the C57Bl/6 background. These inbred mice have a homogeneous genetic background compared to outbred strains such as the CD-1 background. Previous studies have shown that a particular allele may yield a more or less severe phenotype, even sometimes a different phenotype, when placed into a different strain background (examples: *Memo1*,[43] *Tcof1*,[44] *Tgfb3*,[45] *Spry*[46]). Therefore, it is possible that *Mafb* mutations could lead to a craniofacial phenotype on an alternative, cleft-susceptible genetic background.

MAFB belongs to the MAF family of transcription factors, which consists of both large (including MAFB and c-MAF) and small MAFs. Among the large MAF members, MAFB and c-MAF share related binding motifs and biological function.[19] For example, both c-MAF and MAFB are detected in differentiated keratinocytes of the skin. Importantly, the effect on epidermal differentiation was stronger when both *c-MAF* and *MAFB* were knocked out compared to individually.[19] In another context, during neurogenesis, c-MAF and MAFB had redundant functions to generate the proper numbers of GABAergic interneurons.[31] Therefore, it is possible that loss of *Mafb* in the mouse is functionally compensated by another Maf family member during palatogenesis. Expression profiling on epithelial tissue of $Mafb^{del/del}$ did not reveal changes in other MAF family member (Table 2), although we cannot rule out that functional compensation, without changes in expression level, did not occur.

Mice are powerful animal models for human diseases, but do not always present with the same phenotype as humans even with equivalent genetic modifications. For example, mutations in *PVRL1* can contribute to cleft lip and palate and ectodermal dysplasia syndrome, which can include cleft lip and palate among other defects. However, mice lacking this gene develop eye and tooth enamel defects.[47] Also, genetic manipulation of genes causing both cleft lip and palate in humans often result in cleft palate only in mice due to differences in craniofacial morphology (i.e., *Arhgap29*, *FoxE1*, *Irf6*). Finally, not all the molecules involved in cleft palate in mice are correlated with cleft lip and/or palate in humans.[48]

Despite these drawbacks, the mouse is still one of the best animal models to functionally validate genetic findings related to human diseases. It allows us to better understand stages of disease, early pathogenesis, test drugs, and therapies, and contribute to our understanding of the link between a mutant gene and an abnormal phenotype. Different alleles may yield different phenotypes, which can enhance our understanding of the function of a gene in different tissues. Our studies have shed the light on *Mafb* which we have found dispensable for palatogenesis in the mouse, leading us to wonder whether *MAFB* is the etiologic gene contributing to cleft lip and palate at the 20q chromosomal locus in humans. While this locus is frequently associated with orofacial clefting, it may contribute to palatogenesis in conjunction with other variations in the genome that remain to be elucidated.

4 | EXPERIMENTAL PROCEDURES

4.1 | Creation of the Mafb mutant alleles

A 12.2 Kb genomic fragment containing the entire mouse *Mafb* gene was isolated from a C57BL/6J BAC library and cloned into a pgk-DTA targeting vector. A single C to G base change was engineered by site-directed mutagenesis at position 782 of the gene, resulting in an H to Q amino acid change at position 131, replicating the human mutation (Figure 1A,B). In addition, a single loxP site was placed ~900 bp upstream of the transcriptional start site in non-conserved sequence. A FRT-neo-FRT-loxP cassette was inserted just 3′ to the *Mafb* untranslated sequence for positive selection in ES cells. The construct was targeted to C57BL/6J (JM8) ES cells and three clones injected into B6(Cg)-$^{Tyrc\text{-}2J}$/J (JAX Stock #0058) host blastocysts. Germline transmission was confirmed by genotyping for both

loxP sites and sequencing of the point mutation. The line was bred to Flpe-expressing mice (JAX Stock #9086) to remove the neo cassette, and the resulting mice were intercrossed as described in this study. The line was maintained on a C57BL/6J genetic background.

4.2 | Generation and processing of embryos

This procedure was approved by The Jackson Laboratory's Animal Care and Use Committee under the NIH guidelines for the humane care and use of laboratory research animals. It conformed with ARRIVE guidelines for animal studies.

Animals were mated overnight and inspected the following morning for the presence of a vaginal plug (= embryonic day [e] 0.5). Pregnant females were euthanized via CO_2. Litters were dissected at e9.5, e14.5, e18.5, fixed with 4% paraformaldehyde, and embedded in paraffin for histology. Seven micrometer serial sections were collected on slides, then stained with hematoxylin and eosin.

Tissue was submitted to The Jackson Laboratory's Transgenic Genotyping Service for genotyping with ARMS PCR, with primer sequences 5′-GAGCCACTGAGTGCACAGAC-3′ (F post-cre), 5′-AACTAGCAGCCCAGTCCTGA-3′ (R post-cre), and 5′-CAAACGCTCCCAAAGAAGAT-3′ (R2 post-cre). Genotypes were verified with Sanger sequencing.

4.3 | RNA extraction and sequencing

Embryonic skin at e18.5 was isolated and flash frozen. Organic RNA extraction with a Qiagen RNAeasy kit cleanup was performed by the University of Wisconsin Biotechnology Center Gene Expression Center. RNA quantity and RIN was measured by NanoDrop One and Agilent RNA NanoChip. RNA was submitted to the Genomics Division of the Iowa Institute of Human Genetics for library preparation using Illumina TruSeq Stranded Total RNA with Ribozero gold and sequencing on Illumina HiSeq 4000 75 PE. Sequencing reads were submitted to the Bioinformatics Division of the Iowa Institute of Human Genetics for analysis.

4.4 | Measurement of oral adhesions

Oral adhesions were assessed on coronal sections and defined as regions of the oral cavity with contact between opposing epithelia. They were measured spatially in the x/y and z directions. Oral adhesions in the x/y directions were measured as previously described.[35,37] A representative section was selected on which the length of the maxillary epithelium was measured and compared with the length of the maxillary epithelium in contact with opposing structures. Percentage of oral epithelium in contact was calculated and compared between genotypes. One-way ANOVA was used to determine statistical significance between groups.

4.5 | Fluorescent immunostaining

Immunostaining was performed as previously described.[49] Primary antibodies used were: anti-mouse keratin 6 (Covance, Emeryville, California, cat#PRB-169P), anti-human p63 (Santa Cruz, Dallas, Texas, cat#sc8431), and anti-human E-cadherin (BD Transduction

Laboratories, San Jose, California, cat#610182). Secondary antibodies were: Alexa Fluor 488 anti-mouse IgG (Invitrogen, Carlsbad, California cat #A-11017), Alexa Fluor 568 anti-rabbit IgG (Invitrogen, Carlsbad, California, cat#A-11004). Nuclear DNA was labeled with DAPI (4′,6-diamidino-2-phenylindole). Mountant was ProLong Diamond containing DAPI (Life Technologies, Eugene, Oregon). Immunofluorescent images were acquired with a Zeiss 700 Confocal, processed using NIH Image J and presented as maximum projection of two to four confocal slices.

4.6 | DNA cloning, cell culture, transient transfection, and luciferase assay

The human MAFB and mutated MAFB H131Q expression vectors were purchased from Genscript (Accession No. NM_005461.4) in pcDNA3.1(+) and mutation verified by Sanger sequencing. ARHGAP29 enhancer luciferase vectors (pGL3-PROMOTER) were a gift from Robert Cornell.[39] pGL3-basic-ARHGAP29 promoter was a gift from Marius Sudol (Addgene plasmid # 104155; http://n2t.net/addgene:104155; RRID:Addgene_104155).[50] Using previously reported MAFB ChIP-seq data[19] an MAFB binding site in the ARHGAP29 promoter was identified. To engineer the mutated ARHGAP29 promoter plasmid, the MAFB ChIP-seq peak and seven surrounding base pairs were deleted from the Arhgap29 luciferase promoter vector using Around-the-Horn mutagenesis. The mutated plasmid was then amplified following the Phusion High-Fidelity DNA Polymerase protocol (New England Biolabs Inc., Ipswitch, Massachusetts) using 5′-GGGACAGCGTCCGGCCGC-3′ and 5′-GGGCTGCGTCGGCTGCCC-3′ primers, phosphorylated with T4 DNA Ligase buffer and T4 PNK for 30 minutes at 37°C, and ligated with T4 DNA ligase for 2 hours at room temperature. Mutagenesis was confirmed by Sanger sequencing.

LS-8, murine ectodermal-derived enamel producing cells,[51] were cultured in DMEM supplemented with 10% fetal calf serum and 1% penicillin/streptomycin. HEPM cells were cultured in DMEM supplemented with 10% fetal bovine serum and 1% penicillin/streptomycin. HEPM and LS-8 were seeded in 24-well plates and transfected when about 40% and 20% confluency, respectively, using GenePORTER transfection reagent (Genlantis, San Diego, California). Cells were resuspended in OPTIMEM with 263 ng of expression plasmid (or empty plasmid as a control), 188 ng of reporter plasmid and 50 ng of SV-40 beta-galactosidase plasmid with three technical replicates per experiment. Following a 48 hours incubation, transfected cells were lysed and assayed for reporter activities (luciferase assay, Promega, Fitchburg, Wisconsin) and beta-galactosidase activity (Galacto-Light Plus reagents, Tropix Inc.). All luciferase values were normalized to beta-galactosidase activity and displayed as a mean-fold change relative to control condition (empty expression plasmid + reporter plasmid). Results from three separate experiments were analyzed by One-way ANOVA to determine statistical significance.

ACKNOWLEDGMENTS

The authors would like to thank Dr. Brian Schutte for critical reading of the manuscript and the Craniofacial Interest Group for continuous feedback. The authors would like to thank Dr. Bahri Karacay for initial conversation about the H131Q functional assessment, Steve Eliason and Dr. Brad Amendt for technical help with luciferase assays, use of their luminometer and gift of the LS-8 cells, and Dr. Rob Cornell for sharing the ARHGAP29 enhancer constructs. A special thanks to Dr. Eric Van Otterloo for his generous help with RNA sequencing analysis. We

also thank the University of Wisconsin Biotechnology Center Gene Expression Center for RNA extraction. Data presented herein were obtained at the Genomics Division (library prep and RNA-seq) and Bioinformatics Division (RNA-seq analysis) of the Iowa Institute of Human Genetics which is supported, in part, by the University of Iowa Carver College of Medicine. Brian Paul and Melissa Carlson were recipients of a fellowship from the Iowa Center for Undergraduate Research. This work was supported by NIH-AR067739 to M.D. and additional partial financial support was provided by a grant from the National Institute of Health R37DE08559 and by the FaceBase consortium (grants DE020052 and DE020057).

Funding information

National Institute of Health (NIH), Grant/Award Numbers: AR067739, DE020052, DE020057

REFERENCES

1. Dixon MJ, Marazita ML, Beaty TH, Murray JC. Cleft lip and palate: understanding genetic and environmental influences. Nat Rev Genet. 2011;12(3):167–178. 10.1038/nrg2933. [PubMed: 21331089]
2. Leslie EJ, Marazita ML. Genetics of cleft lip and cleft palate. Am J Med Genet C Semin Med Genet. 2013;163C(4):246–258. 10.1002/ajmg.c.31381. [PubMed: 24124047]
3. Li C, Lan Y, Jiang R. Molecular and cellular mechanisms of palate development. J Dent Res. 2017;96(11):1184–1191.10.1177/0022034517703580 [PubMed: 28745929]
4. Moreno LM, Mansilla MA, Bullard SA, et al. FOXE1 association with both isolated cleft lip with or without cleft palate, and isolated cleft palate. Hum Mol Genet. 2009;18(24):4879–4896. 10.1093/hmg/ddp444. [PubMed: 19779022]
5. Butali A, Suzuki S, Cooper ME, et al. Replication of genome wide association identified candidate genes confirm the role of common and rare variants in PAX7 and VAX1 in the etiology of nonsyndromic CL(P). Am J Med Genet A. 2013;161A(5):965–972. 10.1002/ajmg.a.35749. [PubMed: 23463464]
6. Birnbaum S, Ludwig KU, Reutter H, et al. Key susceptibility locus for nonsyndromic cleft lip with or without cleft palate on chromosome 8q24. Nat Genet. 2009;41(4):473–477. 10.1038/ng.333. [PubMed: 19270707]
7. Beaty TH, Murray JC, Marazita ML, et al. A genome-wide association study of cleft lip with and without cleft palate identifies risk variants near MAFB and ABCA4. Nat Genet. 2010;42(6): 525–531. 10.1038/ng.580. [PubMed: 20436469]
8. Leslie EJ, Carlson JC, Shaffer JR, et al. A multiethnic genome-wide association study identifies novel loci for non-syndromic cleft lip with or without cleft palate on 2p24.2, 17q23 and 19q13. Hum Mol Genet. 2016;25(13):2862–2872. 10.1093/hmg/ddw104. [PubMed: 27033726]
9. Leslie EJ, Liu H, Carlson JC, et al. A genome-wide association study of nonsyndromic cleft palate identifies an etiologic missense variant in GRHL3. Am J Hum Genet. 2016;98(4):744–754. 10.1016/j.ajhg.2016.02.014. [PubMed: 27018472]
10. Butali A, Mossey PA, Adeyemo WL, et al. Genomic analyses in African populations identify novel risk loci for cleft palate. Hum Mol Genet. 2019;28(6):1038–1051. 10.1093/hmg/ddy402. [PubMed: 30452639]
11. Ludwig KU, Mangold E, Herms S, et al. Genomewide meta-analyses of nonsyndromic cleft lip with or without cleft palate identify six new risk loci [Research Support, Non-U.S. Gov't]. Nat Genet. 2012;44(9):968–971. 10.1038/ng.2360. [PubMed: 22863734]
12. Huang L, Liang X, Ou Y, Tang S, He Y. Association between 20q12 rs13041247 polymorphism and risk of nonsyndromic cleft lip with or without cleft palate: a meta-analysis. BMC Oral Health. 2020;20(1):39. 10.1186/s12903-020-1003-2. [PubMed: 32019513]
13. Zhang B, Duan S, Shi J, et al. Family-based study of association between MAFB gene polymorphisms and NSCL/P among Western Han Chinese population. Adv Clin Exp Med. 2018;27 (8):1109–1116. 10.17219/acem/74388. [PubMed: 30024657]
14. Imani MM, Lopez-Jornet P, Pons-Fuster Lopez E, Sadeghi M. Polymorphic variants of V-Maf Musculoaponeurotic Fibrosarcoma oncogene homolog B (rs13041247 and rs11696257) and risk of non-Syndromic cleft lip/palate: systematic review and meta-analysis. Int J Environ Res Public Health. 2019;16(15): 2792–2805. 10.3390/ijerph16152792.

15. Moreno Uribe LM, Fomina T, Munger RG, et al. A population-based study of effects of genetic loci on Orofacial clefts. J Dent Res. 2017;96(11):1322–1329. 10.1177/0022034517716914. [PubMed: 28662356]
16. Yin X, Ma L, Li Y, et al. Genetic variants of 20q12 contributed to non-syndromic orofacial clefts susceptibility. Oral Dis. 2017; 23(1):50–54. 10.1111/odi.12570. [PubMed: 27537108]
17. Adzhubei IA, Schmidt S, Peshkin L, et al. A method and server for predicting damaging missense mutations. Nat Methods. 2010;7(4):248–249. 10.1038/nmeth0410-248. [PubMed: 20354512]
18. Cordes SP, Barsh GS. The mouse segmentation gene kr encodes a novel basic domain-leucine zipper transcription factor. Cell. 1994;79(6):1025–1034. 10.1016/0092-8674(94)90033-7. [PubMed: 8001130]
19. Lopez-Pajares V, Qu K, Zhang J, et al. A LncRNA-MAF:MAFB transcription factor network regulates epidermal differentiation. Dev Cell. 2015;32(6):693–706. 10.1016/j.devcel.2015.01.028. [PubMed: 25805135]
20. Artner I, Blanchi B, Raum JC, et al. MafB is required for islet beta cell maturation. Proc Natl Acad Sci U S A. 2007;104(10): 3853–3858. 10.1073/pnas.0700013104. [PubMed: 17360442]
21. Aziz A, Vanhille L, Mohideen P, et al. Development of macrophages with altered Actin organization in the absence of MafB. Mol Cell Biol. 2006;26(18):6808–6818. 10.1128/MCB.00245-06. [PubMed: 16943423]
22. Blanchi B, Kelly LM, Viemari JC, et al. MafB deficiency causes defective respiratory rhythmogenesis and fatal central apnea at birth. Nat Neurosci. 2003;6(10):1091–1100. 10.1038/nn1129. [PubMed: 14513037]
23. Li MA, Alls JD, Avancini RM, Koo K, Godt D. The large Maf factor traffic jam controls gonad morphogenesis in drosophila. Nat Cell Biol. 2003;5(11):994–1000. 10.1038/ncb1058. [PubMed: 14578908]
24. Moriguchi T, Hamada M, Morito N, et al. MafB is essential for renal development and F4/80 expression in macrophages. Mol Cell Biol. 2006;26(15):5715–5727. 10.1128/MCB.00001-06. [PubMed: 16847325]
25. Sadl V, Jin F, Yu J, et al. The mouse Kreisler (Krml1/MafB) segmentation gene is required for differentiation of glomerular visceral epithelial cells. Dev Biol. 2002;249(1):16–29. 10.1006/dbio.2002.0751. [PubMed: 12217315]
26. Rondon-Galeano M, Skoczylas R, Bower NI, et al. MAFB modulates the maturation of lymphatic vascular networks in mice. Dev Dyn. 2020;249(10):1201–1216. 10.1002/dvdy.209. [PubMed: 32525258]
27. Hertwig P. Neue Mutationen und Koppelungsgruppen bei der Hausmaus. ZIAV. 1942;80:220–246.
28. Manzanares M, Cordes S, Kwan CT, Sham MH, Barsh GS, Krumlauf R. Segmental regulation of Hoxb-3 by kreisler. Nature. 1997;387(6629):191–195. 10.1038/387191a0. [PubMed: 9144291]
29. Tani-Matsuhana S, Vieceli FM, Gandhi S, Inoue K, Bronner ME. Transcriptome profiling of the cardiac neural crest reveals a critical role for MafB. Dev Biol. 2018;444:17. 10.1016/j.ydbio.2018.09.015.
30. Chen J, Du Y, He X, Huang X, Shi YSA. Convenient Cas9-based conditional knockout strategy for simultaneously targeting multiple genes in mouse. Sci Rep. 2017;7(1):517. 10.1038/s41598-017-00654-2. [PubMed: 28364122]
31. Pai EL, Vogt D, Clemente-Perez A, et al. Mafb and c-Maf have prenatal compensatory and postnatal antagonistic roles in cortical interneuron fate and function. Cell Rep. 2019;26(5):1157–1173e5. 10.1016/j.celrep.2019.01.031. [PubMed: 30699346]
32. Miyai M, Tsunekage Y, Saito M, Kohno K, Takahashi K, Kataoka K. Ectopic expression of the transcription factor MafB in basal keratinocytes induces hyperproliferation and perturbs epidermal homeostasis. Exp Dermatol. 2017;26(11):1039–1045. 10.1111/exd.13364. [PubMed: 28418611]
33. Sato Y, Tsukaguchi H, Morita H, et al. A mutation in transcription factor MAFB causes focal segmental glomerulosclerosis with Duane retraction syndrome. Kidney Int. 2018;94(2):396–407. 10.1016/j.kint.2018.02.025. [PubMed: 29779709]
34. Park JG, Tischfield MA, Nugent AA, et al. Loss of MAFB function in humans and mice causes Duane syndrome, aberrant extraocular muscle innervation, and inner-ear defects. Am J Hum Genet. 2016;98(6):1220–1227. 10.1016/j.ajhg.2016.03.023. [PubMed: 27181683]

35. Paul BJ, Palmer K, Sharp JC, Pratt CH, Murray SA, Dunnwald M. ARHGAP29 mutation is associated with abnormal oral epithelial adhesions. J Dent Res. 2017;96(11):1298–1305. 10.1177/0022034517726079. [PubMed: 28817352]
36. Ingraham CR, Kinoshita A, Kondo S, et al. Abnormal skin, limb and craniofacial morphogenesis in mice deficient for interferon regulatory factor 6 (Irf6). Nat Genet. 2006;38(11): 1335–1340. [PubMed: 17041601]
37. Kousa YA, Roushangar R, Patel N, et al. IRF6 and SPRY4 signaling interact in periderm development. J Dent Res. 2017;96 (11):1306–1313. 10.1177/0022034517719870. [PubMed: 28732181]
38. Leslie EJ, Mansilla MA, Biggs LC, et al. Expression and mutation analyses implicate ARHGAP29 as the etiologic gene for the cleft lip with or without cleft palate locus identified by genome-wide association on chromosome 1p22 [Research Support, N.I.H., Extramural]. Birth Defects Res A Clin Mol Teratol. 2012;94(11):934–942. 10.1002/bdra.23076. [PubMed: 23008150]
39. Liu H, Leslie EJ, Carlson JC, et al. Identification of common non-coding variants at 1p22 that are functional for nonsyndromic orofacial clefting. Nat Commun. 2017;8:14759. 10.1038/ncomms14759. [PubMed: 28287101]
40. Mehawej C, Courcet JB, Baujat G, et al. The identification of MAFB mutations in eight patients with multicentric carpotarsal osteolysis supports genetic homogeneity but clinical variability. Am J Med Genet A. 2013;161A(12):3023–3029. 10.1002/ajmg.a.36151. [PubMed: 23956186]
41. Schoenfelder S, Fraser P. Long-range enhancer-promoter contacts in gene expression control. Nat Rev Genet. 2019;20(8):437–455. 10.1038/s41576-019-0128-0. [PubMed: 31086298]
42. Uslu VV, Petretich M, Ruf S, et al. Long-range enhancers regulating Myc expression are required for normal facial morphogenesis. Nat Genet. 2014;46(7):753–758. 10.1038/ng.2971. [PubMed: 24859337]
43. Van Otterloo E, Feng W, Jones KL, et al. MEMO1 drives cranial endochondral ossification and palatogenesis. Dev Biol. 2016;415(2):278–295. 10.1016/j.ydbio.2015.12.024. [PubMed: 26746790]
44. Dixon J, Dixon MJ. Genetic background has a major effect on the penetrance and severity of craniofacial defects in mice heterozygous for the gene encoding the nucleolar protein treacle. Dev Dyn. 2004;229(4):907–914. 10.1002/dvdy.20004. [PubMed: 15042714]
45. Proetzel G, Pawlowski SA, Wiles MV, et al. Transforming growth factor beta 3 is required for secondary palate fusion. Nat Genet. 1995;11:409–414. [PubMed: 7493021]
46. Percival CJ, Marangoni P, Tapaltsyan V, Klein O, Hallgrimsson B. The interaction of genetic background and mutational effects in regulation of mouse craniofacial shape. G3 (Bethesda). 2017;7(5): 1439–1450. 10.1534/g3.117.040659. [PubMed: 28280213]
47. Barron MJ, Brookes SJ, Draper CE, et al. The cell adhesion molecule nectin-1 is critical for normal enamel formation in mice. Hum Mol Genet. 2008;17(22):3509–3520. 10.1093/hmg/ddn243. [PubMed: 18703497]
48. Funato N, Nakamura M, Yanagisawa H. Molecular basis of cleft palates in mice. World J Biol Chem. 2015;6(3):121–138. 10.4331/wjbc.v6.i3.121. [PubMed: 26322171]
49. Biggs LC, Naridze RL, DeMali KA, et al. Interferon regulatory factor 6 regulates keratinocyte migration. J Cell Sci. 2014;127(Pt13):2840–2848. 10.1242/jcs.139246. [PubMed: 24777480]
50. Qiao Y, Chen J, Lim YB, et al. YAP regulates Actin dynamics through ARHGAP29 and promotes metastasis. Cell Rep. 2017;19(8):1495–1502. 10.1016/j.celrep.2017.04.075. [PubMed: 28538170]
51. Chen LS, Couwenhoven RI, Hsu D, Luo W, Snead ML. Maintenance of amelogenin gene expression by transformed epithelial cells of mouse enamel organ. Arch Oral Biol. 1992;37(10):771–778. 10.1016/0003-9969(92)90110-t. [PubMed: 1444889]

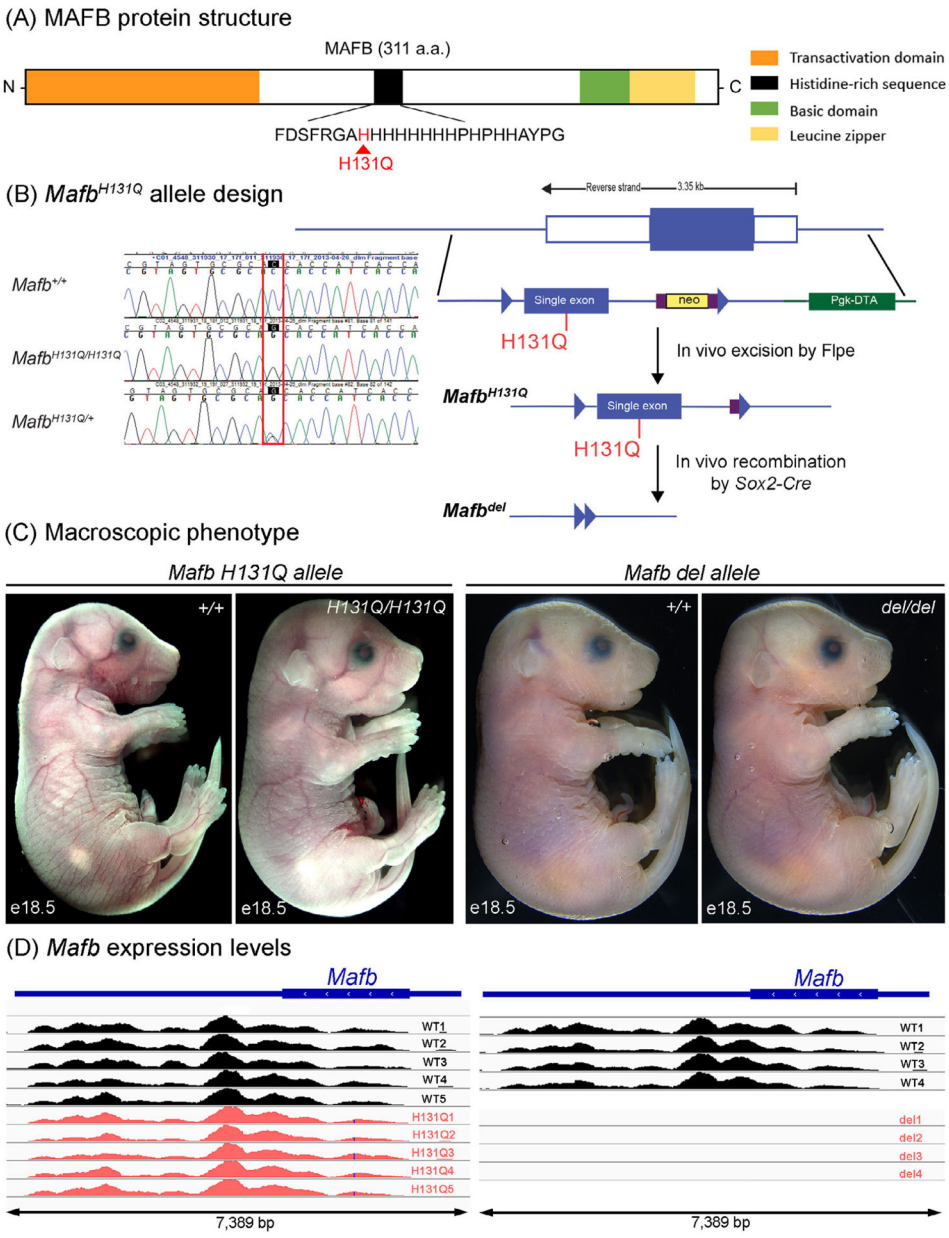

FIGURE 1.

Characterization of the *Mafb* H131Q and del alleles. A, Structure of the MAFB protein, including the histidine-rich domain where the H131Q patient variant is located. B, A single C to G point mutation at position 782 in the single *Mafb* exon identified in human nonsyndromic cleft lip and/or palate patients was engineered into the murine *Mafb*, resulting in protein translation and a substitution of the histidine at position 131 with a glutamine (H131Q). C, The macroscopic phenotypes of e18.5 wild-type and $Mafb^{H131Q/H131Q}$ or wild-type and $Mafb^{del/del}$ embryos have no noticeable difference. D, Visualization of RNA-seq mapping reads for *Mafb* in five wild-type (WT1–5) and five $Mafb^{H131Q/H131Q}$ (H131Q1–5; left panel) and four wild-type (WT1–4), and four $Mafb^{del/del}$ (del1–4; right panel) e18.5

skin. Data were visualized in the UCSC Genome Browser. Vertical axis shows read counts. Map of the single exon organization of the *Mafb* gene is shown on top of the panel

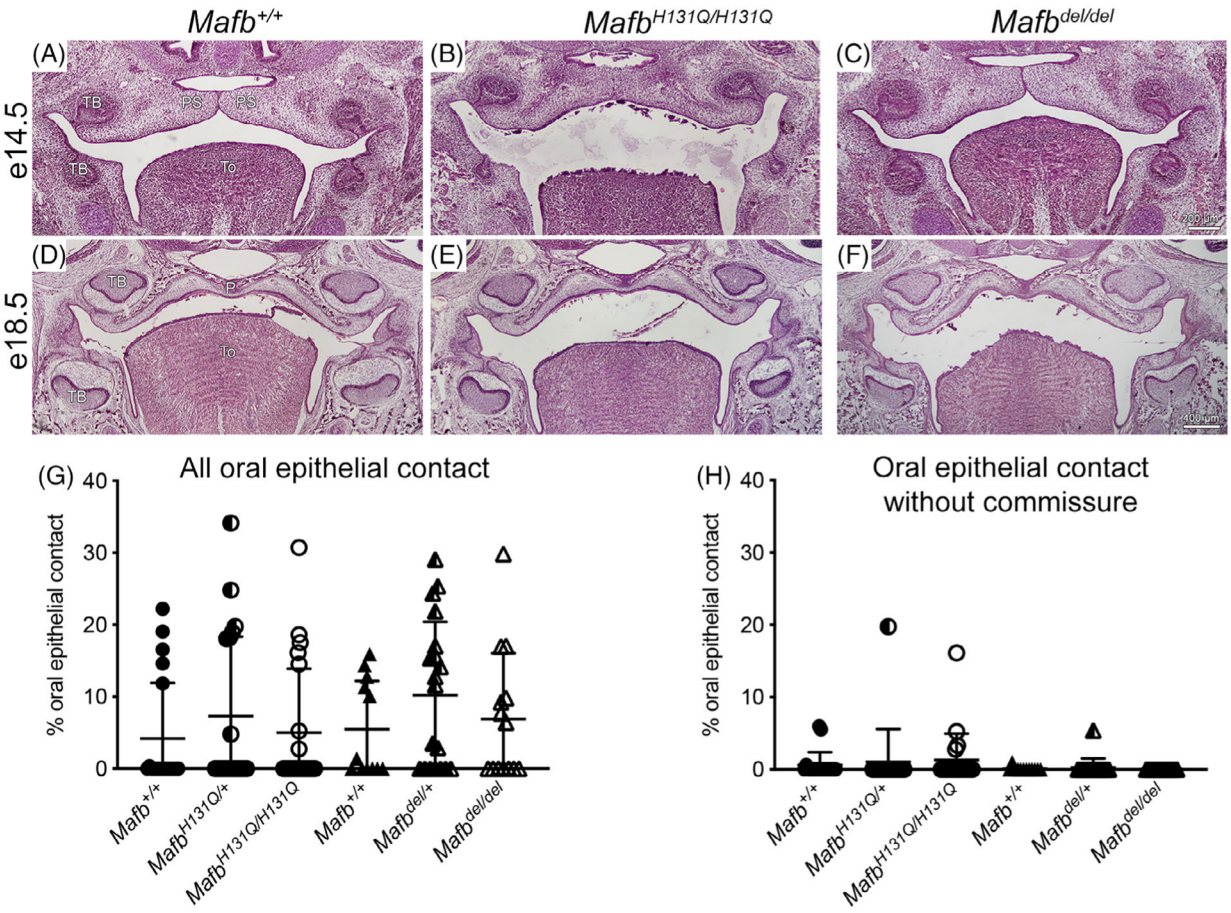

FIGURE 2.

Palatogenesis is not altered in *Mafb*$^{H131Q/H131Q}$ or *Mafb*$^{del/del}$ mice. A-F, Coronal section of wild-type, A, D; *Mafb*$^{H131Q/H131Q}$, B, E; and *Mafb*$^{del/del}$, C, F; murine embryonic heads at e14.5, A-C; and e18.5, D-F. In e14.5, palatal shelves were elevated and made contact at the midline, A-C. In e18.5, palatogenesis is completed with a confluent mesenchymal bridge lined by the oral epithelium, D-F. G, H, Quantification of oral adhesions at both e13.5 and e14.5 (Mafb H131Q line) and e14.5 (Mafb del line) as described in Table 3. Percentage of oral epithelium in contact, G. Percentage of oral epithelium in contact excluding mild contact only in the commissures (H). P, palate; PS, palatal shelf; TB, tooth bud; To, tongue

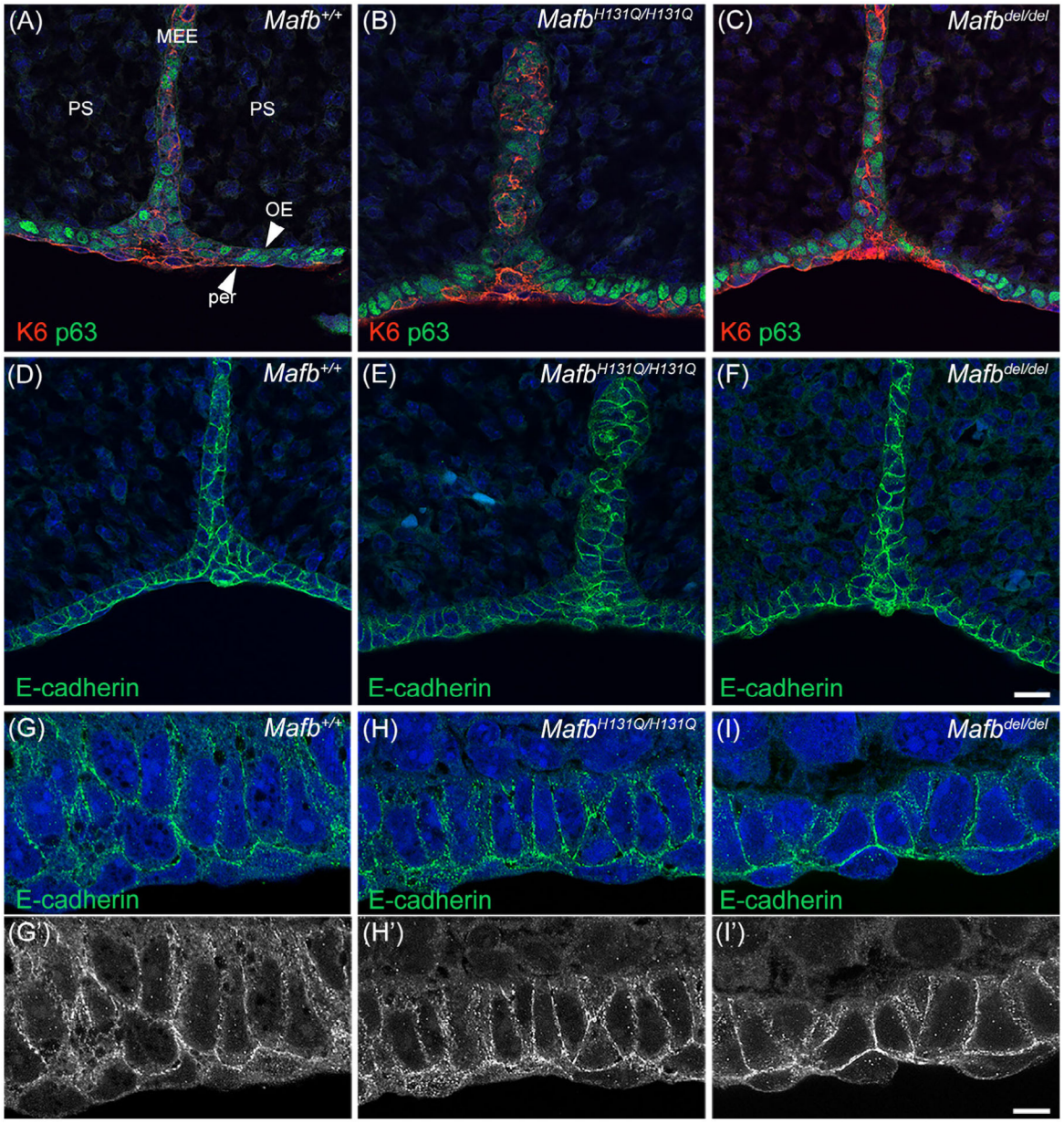

FIGURE 3.

Periderm morphogenesis is not altered in *Mafb*$^{H131Q/H131Q}$ or *Mafb*$^{del/del}$ mice. Coronal section of wild-type, A, D, G, G′; *Mafb*$^{H131Q/H131Q}$, B, E, H, H′; and *Mafb*$^{del/del}$ C, F, I, I′, murine embryonic palates at e14.5 immunostained for keratin 6 (K6) and p63, A-C; and E-cadherin, D-I′. Oral epithelial (K6-negative and p63-positive) and periderm cells (K6-positive and p63-negative) are indicated in (A) by white arrows. Scale bar = 16 μm. G′, H′ and I′ are single channel images of G, H and I (Scale bar = 5 μm). MEE, medial edge epithelium; OE, oral epithelium; per = periderm; PS, palatal shelves

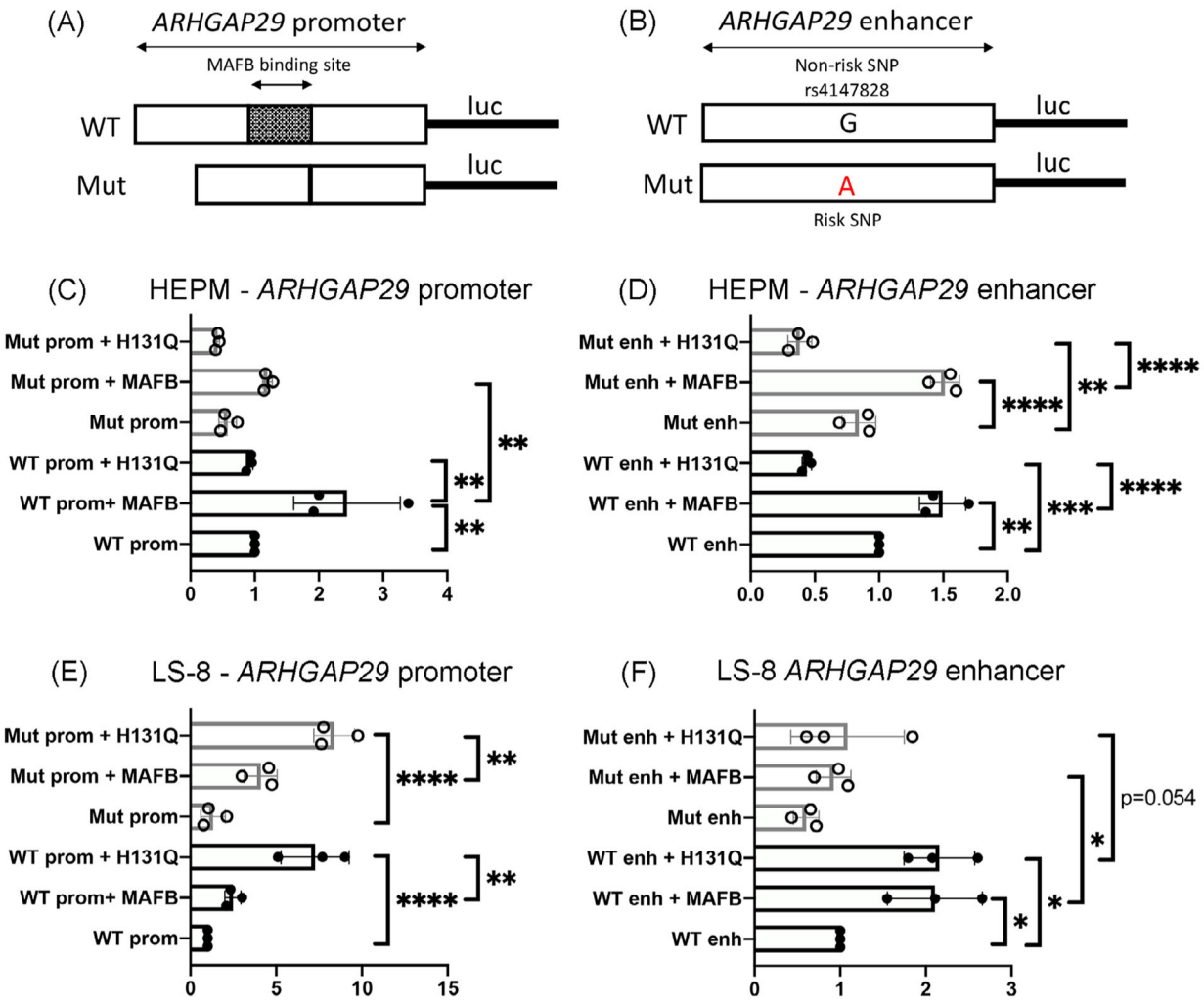

FIGURE 4.

MAFB H131Q alters *ARHGAP29* promoter- and enhancer-driven activity in a cell-dependent context. The *ARHGAP29* promoter, A, C, E, or *ARHGAP29* enhancer, B, D, F was cloned into the luciferase reporter. Deletion of the MAFB binding site in the ARHGAP29 promoter (A) and risk SNPs in the ARHGAP29 enhancer (B) were considered mutant (Mut). Human embryonic palatal mesenchyme (HEPM) cells (C, D) or LS-8 cells (E, F) transfected with the *ARHGAP29* promoter or the *ARHGAP29* enhancer were cotransfected with vector-only plasmid (WT), or plasmids containing wild-type (MAFB) or H131Q variant MAFB (H131Q). Bar chart shows luciferase activity reported as relative to the respective vector-only control. Values are presented as mean SD of three biological replicates. **P* < .05, ***P* < .01, ****P* < .005, *****P* < .0001

TABLE 1

Intercross genotype results

		Number of embryos				
		e9.5 (5 litters)	**e14.5 (15 litters)**	**e18.5 (28 litters)**	**P0**	**Total**
H131Q	*Mafb* $^{+/+}$	10	25	53	Viable	88
	Mafb $^{H131Q/+}$	15	59	98	Viable	172
	Mafb $^{H131Q/H131Q}$	7	34	47	Viable	88
	Genotype ND[a]	10	5	8		23
	Resorption	1	7	4	n/a[b]	12
	Total	42	123	206		371
		Number of embryos				
		e9.5	**e14.5 (15 litters)**	**e18.5 (18 litters)**	**P0 (11 litters)**	**Total**
del	*Mafb* $^{+/+}$	-	27	27	13	67
	Mafb $^{del/+}$	-	55	67	27	149
	Mafb $^{del/del}$	-	22	27	0***	49
	Genotype ND	-	0	1	2	3
	Resorption	-	5	14	-	19
	Total		109	136	42	268

[a] Embryos for which the genotype was not conclusive.

[b] Not applicable.

*** $P < .001$ after Chi-Square compared to expected Mendelian ratios.

TABLE 2

Fold change in expression levels of selected craniofacial and cutaneous genes

	$Mafb^{H131Q/H131Q}$		$Mafb^{del/del}$	
	Fold change [a]	**Adj. *P*-value**	***Fold change*** [b]	**Adj. *P*-value**
Mafb	0.70	.40	−1307****	1.28×10^{-41}
Mafa	0.67	.61	1.08	.99
Maff	0.94	.91	−1.23	.99
Mafg	0.89	.58	−1.14	.39
Mafk	0.86	.58	−1.07	.99
Maf	−1.08	.79	1.09	.99
Arhgap24	0.83	.49	−1.77****	5.13×10^{-15}
Arhgap29	−1.09	.69	1.01	.99
Cdh1	0.87	.65	−1.11	.99
Irf6	0.89	.69	1.12	.99
Trp63	−1.03	.93	−1.03	.99
Krt1	0.72	.62	−3.46****	1.44×10^{-31}
Krt10	0.66	.62	−2.92****	6.84×10^{-09}

[a] Ratios between $Mafb^{+/+}$ and $Mafb^{H131Q/H131Q}$ littermate samples.

[b] Ratios between $Mafb^{+/+}$ and $Mafb^{del/del}$ littermate samples.

**** $P < .0001$.

TABLE 3

Detailed craniofacial phenotype

	Time point	Palatal shelves elevated	Palatal shelves in contact	Commissure contact[a]	Palatal shelf to tongue adhesion	Tooth bud adhesion[b]	Any oral adhesion[c]	Potentially deleterious adhesion[d]
Mafb $^{+/+}$	e13.5	0/2 0%	0/2 0%	0/2 0%	0/2 0%	0/2 0%	0/2 0%	0/2 0%
	e14.5	13/18 72%	11/18 61%	0/18 0%	0/18 0%	0/18 0%	6/18 33%	1/18 5%
Mafb $^{H131Q/+}$	e13.5	0/8 0%	0/8 0%	2/8 25%	0/8 0%	0/8 0%	3/8 38%	2/8 25%
	e14.5	11/18 61%	9/18 50%	0/18 0%	0/18 0%	0/18 0%	3/18 17%	0/18 0%
Mafb $^{H131Q/H131Q}$	e13.5	0/6 0%	0/6 0%	0/6 0%	2/6 33%	1/6 17%	4/6 67%	4/6 67%
	e14.5	11/16 69%	9/16 56%	0/16 0%	1/16 6%	0/16 0%	4/16 25%	1/16 6%
Mafb $^{+/+}$	e14.5	10/13 77%	6/13 46%	0/13 0%	0/13 0%	0/13 0%	5/13 38%	0/13 0%
Mafb $^{del/+}$	e14.5	9/19 47%	6/19 31%	0/19 0%	0/19 0%	1/19 5%	7/19 37%	1/19 5%
Mafb $^{del/del}$	e14.5	9/15 60%	7/15 47%	0/15 0%	0/15 0%	1/15 7%	8/15 53%	1/15 7%

[a] The maxillary and mandibular oral epithelia in the lateral commissure (lateral to the tooth bud) are in contact.

[b] Any instance of adhesion involving the maxilla or mandibular tooth bud with opposing epithelium.

[c] Contact between a maxillary structure (including palatal shelves) and an opposing structure. This includes contact in the commissure only if it extends medially beyond the half-way point between the maxillary and mandibular tooth buds.

[d] The adhesion involves a not-yet elevated palatal shelf and mandibular or lingual epithelium.

TABLE 4

Arhgap29$^{K326/+}$;*Mafb*$^{del/+}$ outcross genotype results

	e14.5 (1 litter)	**e18.5 (3 litters)**	**P0 (6 litters)**	**Total**
Mafb$^{+/+}$;*Arhgap29*$^{+/+}$	3	6	4	13
Mafb $^{del/+}$	4	4	10	18
Arhgap29 $^{K326X/+}$	1	2	7	10
Mafb$^{del/+}$;*Arhgap29*$^{K326X/+}$	1	6	6	13
Genotype ND[a]	-	-	8	8
Resorption	2	2		4
Total	11	20	35	62

[a]Embryos for which the genotype was not conclusive.